### **PAPER**

Substrate dependent electronic structure variations of van der Waals heterostructures of  $MoSe_2$  or  $MoSe_{2(1-x)}Te_{2x}$  grown by van der Waals epitaxy

To cite this article: Horacio Coy Diaz et al 2017 2D Mater. 4 025094

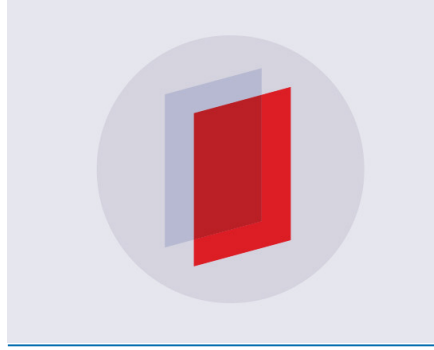
View the article online for updates and enhancements.

### Related content

- Molecular beam epitaxy of the van der Waals heterostructure MoTe2 on MoS2: phase, thermal, and chemical stability
   Horacio Coy Diaz, Redhouane Chaghi, Yujing Ma et al.
- Multimodal spectromicroscopy of monolayer WS2 enabled by ultra-clean van der Waals epitaxy
   C Kastl, C T Chen, R J Koch et al.
- 2D Materials Advances: From Large Scale Synthesis and Controlled Heterostructures to Improved Characterization Techniques. Defects and Applications
   Zhong Lin, Amber McCreary, Natalie Briggs et al.

### Recent citations

- Electronic Properties of Transferable Atomically Thin MoSe2/h-BN Heterostructures Grown on Rh(111) Ming-Wei Chen et al
- <u>Telluride-Based Atomically Thin Layers of</u> <u>Ternary Two-Dimensional Transition Metal</u> <u>Dichalcogenide Alloys</u> <u>Amey Apte *et al*</u>
- <u>Unraveling the Structural and Electronic</u> <u>Properties at the WSe2–Graphene</u> <u>Interface for a Rational Design of van der</u> <u>Waals Heterostructures</u> <u>Stefano Agnoli et al</u>



## IOP ebooks™

Bringing you innovative digital publishing with leading voices to create your essential collection of books in STEM research.

Start exploring the collection - download the first chapter of every title for free.

### **2D** Materials



RECEIVED 15 March 2017

REVISED

10 April 2017

ACCEPTED FOR PUBLICATION 21 April 2017

PUBLISHED 5 May 2017

### **PAPER**

# Substrate dependent electronic structure variations of van der Waals heterostructures of $MoSe_2$ or $MoSe_{2(1-x)}Te_{2x}$ grown by van der Waals epitaxy

Horacio Coy Diaz<sup>1</sup>, Yujing Ma<sup>1</sup>, Sadhu Kolekar<sup>1</sup>, José Avila<sup>2,3</sup>, Chaoyu Chen<sup>2,3</sup>, Maria C Asensio<sup>2,3</sup> and Matthias Batzill<sup>1</sup>

- Department of Physics, University of South Florida, Tampa, FL 33647, United States of America
- Synchrotron SOLEIL, L'Orme des Merisiers, Saint Aubin-BP 48, Gif sur Yvette Cedex 91192, France
- <sup>3</sup> Université Paris-Saclay, L'Orme des Merisiers, Saint Aubin-BP 48, Gif sur Yvette Cedex 91192, France

E-mail: mbatzill@usf.edu

Keywords: heterostructure, interface, electronic structure

#### **Abstract**

Substrate induced variation of the electronic structure of MoSe<sub>2</sub> monolayers is studied. MoSe<sub>2</sub> is directly grown by van der Waals epitaxy on MoS<sub>2</sub> and highly ordered pyrolytic graphite (HOPG). In this article, we give a review of growth of transition metal dichalcogenides (TMDCs) by van der Waals epitaxy and discuss previously found evidence for the modifications of the electronic structure of TMDCs by van der Waals substrates. Using angle resolved photoemission spectroscopy and scanning tunneling microscopy/spectroscopy we determine the dispersion of the valence band and the band gap, respectively. For MoSe<sub>2</sub> on graphite the valence band resembles that expected for free standing single layer MoSe<sub>2</sub>, however, the substrate induces a narrowing of the overall band gap. For MoSe<sub>2</sub> on MoS<sub>2</sub> evidence for hybridization of the valence band maximum between the monolayer and the substrate are presented. Such hybridization, results in an alignment of the valence band maximum (VBM) of MoSe<sub>2</sub> with the binding energy of the VBM of the MoS<sub>2</sub>-substrate at the  $\Gamma$ -point. Furthermore, the VBM at the  $\Gamma$ -point is very close in energy to that of the VBM at the K-point. The effective electron mass around the  $\Gamma$ -point is also much decreased for MoSe<sub>2</sub> on MoS<sub>2</sub>- compared to HOPG-substrates or free standing MoSe<sub>2</sub> monolayers. This indicates that in TMDC heterostructures interlayer interactions significantly modify the electronic structure and the resulting properties are in between those of free-standing monolayer and bulk materials. In an attempt to control the electronic states incorporation of Te by formation of  $MoSe_{2(1-x)}Te_{2x}$  has been investigated. While shifts in the core level position are observed, the VBM states are found to be very similar to those of pure MoSe<sub>2</sub>.

### 1. Introduction

Van der Waals heterostructures promise to enable the combination of diverse materials with atomically sharp interfaces [1,2]. The weak interlayer interactions suggest that very different materials can be stacked or grown on top of each other with disregard of lattice-matching conditions that are otherwise limiting the material combination for high quality epitaxial films of '3D' materials [3].

The research in van der Waals heterostructures has received renewed interest since the advent of mechanical exfoliation of single- or few-layer materials and their 'arbitrary' reassembling into heterostructures [4]. This relatively simple and inexpensive approach led to the

discovery of fundamental physical behaviors [5–7], proof-of-principle device fabrications [8–13], and characterization of optical responses in van der Waals heterostructures [14–19]. At the same time efforts are underway to directly grow van der Waals heterostacks [20–37] and their lateral heterojunctions [38, 39]. The two main growth methods are chemical vapor deposition (CVD) and molecular beam epitaxy (MBE) [1,40]. Advantages of CVD growth are the lower cost, as well as the larger achievable grains and possibly lower defect concentrations enabled by the higher growth temperatures and pressures in CVD compared to MBE. MBE may, however, have advantages in the relative easy combination of materials, doping, formation of alloys, and growth of chemically less stable van der Waals materials,

which require ultra-high vacuum (UHV) conditions for growth and handling, i.e. generally MBE is more flexible. In this article, we review the initial work done as early as the 1990's on van der Waals epitaxy. Then we highlight key aspects developed recently on how the properties in van der Waals heterostructures are modified from those of single component bulk materials and/or the properties of free-standing single monolayers. This review is followed by original work on MBE grown MoSe<sub>2</sub> and mixed MoSe<sub>x</sub>Te<sub>2-x</sub> monolayer materials supported on MoS<sub>2</sub> and highly ordered pyrolytic graphite (HOPG).

# 2. Brief review of van der Waals epitaxy and properties of van der Waals heterostructures

Van der Waals epitaxy [3, 41] is not a new concept but has attracted renewed interest in recent years. Van der Waals epitaxy refers to the crystallographically aligned growth of layered materials on a substrate, where the two materials may be exhibiting a large lattice mismatch. In this context, we call layered materials any material that exhibits strong in-plane covalent and ionic bonding and only weak, mostly van der Waals interactions between its layers. The substrate may be another layered, 'van der Waals' material, or the surface of a 'bulk-3D' material. Here, we are concerned with van der Waals heterostructures, i.e. systems where the growth substrate is also a layered material and thus we exclusively discuss purely van der Waals heterostructures. Although the main point of van der Waals epitaxy is that the weak interaction between the grown layer and the substrate results in no forced registry of the overlayer onto the substrate lattice, i.e. both the substrate and the overlayer maintain their bulk lattice constants, it is called 'epitaxy' because the grown film has a rotational registry with the substrate. Thus, all nucleated grains should have the same crystallographic orientation so that, in an ideal case, a single domain epitaxial film is formed upon coalescence of the grains.

Early studies of van der Waals heterostructures were primarily conducted in Japan by the Koma-group and in Germany by the Jaegermann-group. In these studies a variety of layered transition metal dichalcogenides (TMDCs) and post-transition metal (In,Sn,Ga) selenides were grown on bulk van der Waals substrates by MBE or metalorganic vapor deposition [42–47]. One point of interest was the interlayer band alignment and formation of quantum well states in such atomically sharp interfaces with weak chemical interactions [48–52]. In these studies the band alignment was mainly characterized by photoemission spectroscopy. Noteworthy is an angle resolved photoemission study that demonstrated the change of band structure of WS2 as a function of layers [53]. In this study WS2 was grown on HOPG and it was observed that for monolayer WS<sub>2</sub> the valence band maximum is located at the K-point and not at the  $\Gamma$ -point as in the bulk. This drastic change in the electronic structure was correctly interpreted as a consequence of the interlayer interaction. This work did not receive much interest in 2001 when it was published. Only the recent optical photoluminescence measurements on TMDCs that demonstrated the transition from an indirect- to a direct- band gap semiconductor, as TMDC is thinned to single layer by mechanical exfoliation [54], renewed the interest in the direct measurement of k-space resolved band structure of TMDCs. NanoARPES studies in a photoemission electron microscope (PEEM) on exfoliated flakes [55] as well as ARPES studies of TMDCs grown by MBE on graphene [56, 57] have been performed and are in agreement with the earlier studies. The effects of interlayer interaction in TMDCs on their electronic structure may be divided into two aspects. One effect is due to the interaction of the frontal orbitals between layers, which are commonly the chalcogen p-orbitals, causing a variation of the part of the valence band that is p-derived [58,59]. For Mo- and W- chalcogenides these are the states at the  $\Gamma$ -point. Consequently, for monolayer the binding energy of the valence band maximum at the  $\Gamma$ -point is increased, and thus moving the valence band maximum (VBM) from the  $\Gamma$ -point in bulk or bi-layer materials to the K-point for the monolayer. Another effect is observed in heterostructures of van der Waals materials in particular TMDCs on conducting substrates, i.e. materials with free charge carriers. In such heterostructures it has been observed that screening effects by the substrate electrons can modify the electronic structure of the TMDCs [60–63]. In particular, such screening will result in a band renormalization which causes a narrowing of the band gap of the TMDCs. In addition to these interlayer interactions, quantum confinement effects in monolayers become important that results in a widening of the band gap for monolayers compared to bulk materials [64].

The aforementioned interlayer orbital interactions reshape the electronic and optical properties for monolayers compared to bulk materials. However, it may also be important in heterostructures when two dissimilar TMDCs are being combined. In heterostructures some interaction between the frontal orbitals is still expected and thus these interactions should modify the electronic structure compared to free-standing monolayers. However, while in a homostructure the spatial relationship between orbitals of the two layers are all the same, in heterostructures the lattice mismatch between the individual layers gives a variety of relative spatial relationships of frontal orbitals from the two layers. In general, lattice mismatched 2D materials will form a moiré structure, where the relative atom positions between the two layers varies within the moiré unit cell. The formation of moiré unit cells in van der Waals epitaxy was first reported from low energy electron diffraction (LEED) for WS<sub>2</sub>/ MoTe<sub>2</sub>(0001) [65]. Since then, moiré structures have been observed in STM studies of TMDCs grown on various van der Waals substrates. The variation of the coordination between the atoms in two layers within the moiré unit cell thus suggests that the electronic structure may

also be modulated within the unit cell. Density functional theory calculations have shown that, depending on the interlayer coordination such an electronic structure modulation should exist [66, 67]. Recent scanning tunneling spectroscopy (STS) on a MoS<sub>2</sub>/WSe<sub>2</sub> heterostructure has shown that the electronic structure for such a TMDC heterostructure is indeed modified with a variation amplitude of 0.15 eV for the band gap within the moiré unit cell [68]. In another recent study, micro ARPES was used to characterize the interlayer hybridization in MoSe<sub>2</sub>/WSe<sub>2</sub> heterostructures fabricated by mechanical exfoliation and careful alignment of the monolayer flakes [69]. Evidence of hybridization in the heterostructure at the  $\Gamma$ -point was found. In addition to the bands that were assigned to monolayer MoSe<sub>2</sub> and WSe<sub>2</sub>, a third band was observed. This new band has been assigned to interlayer hybridization. It was suggested that this hybridization occurs in commensurate regions while the pure monolayer bands are observed in regions where the two layers are incommensurate. Although the observed hybridization band is at lower binding energy than the valence band maxima of the monolayer materials, it is still at a slightly higher binding energies than the valence band maximum at K. Thus, the heterostructure of MoSe<sub>2</sub>/ WSe<sub>2</sub> remains a direct band gap material. In summary, both recent STS and micro-ARPES studies on TMDCs heterostructures demonstrate that a naïve picture for van der Waals heterostructures that describes the electronic structure as the sum of the properties of the individual layers, does not hold. Instead the properties of heterostructures are modified by interlayer interactions. This should also be observed in directly grown TMDC heterostructures by MBE, while TMDCs grown on non-TMDCs, like HOPG, should not exhibit the same hybridization effects at the  $\Gamma$  point of the TMDCs. Generally speaking, interlayer hybridization can only be observed where orbitals overlap in momentum and energy which enables hybridization at the  $\Gamma$  point of two TMDCs, but gives rise to different hybridization effects in very dissimilar materials such as graphene/TMDCs [70].

Here we investigate the properties of MBE grown  $MoSe_2$  monolayers. We find strong dependence of the electronic structure of  $MoSe_2$  on the substrates. In particular, we find evidence of the VBM to be energetically aligned to the VBM of the substrate at the  $\Gamma$  point if grown on another TMDC (i.e.  $MoS_2$ ). Furthermore, the band dispersion at the  $\Gamma$  point is modified for monolayers on  $MoS_2$  compared to HOPG substrates, with the former exhibiting more 'bulk' like dispersion and the latter more 'monolayer' like dispersion. We also expand our studies to selenide/telluride alloys and investigate the formation of  $MoSe_{2(1-x)}Te_{2x}$  solid solutions by MBE.

### 3. Experimental methods

All the experiments were conducted in UHV. The substrates for growth of  $MoSe_2$  or  $MoSe_{2(1-x)}Te_{2x}$  were commercial HOPG, and synthetically grown single crystalline  $MoS_2$ . These substrates were cleaved in air

and immediately introduced into the vacuum chamber. The growth chamber had a base pressure of  $10^{-9}$  Torr. Before growth, the substrates were outgassed for 4h at 300 °C. For growth of mono- to few-layer films, Mo was evaporated from a home-built water-cooled e-beam evaporator. For the evaporant a 2 mm diameter, high purity Mo-rod was used. Atomic selenium was supplied by a valved, hot-wall selenium cracker source, while tellurium was evaporated from a water-cooled effusion cell. The films were grown with chalcogen flux 10 times higher than that of molybdenum flux, at a growth temperature of 300 °C. The growth rate was controlled to be slow with about 1 h for a monolayer. The growth rate varied slightly for different substrates, suggesting that the sticking of the Mo-containing precursors may be different on different substrates. Particularly for HOPG the growth rate was only about 34 that for the growth on MoS<sub>2</sub> substrates under otherwise identical growth conditions.

After completion of the growth, the sample was transferred in situ to the analysis chamber with help of a magnetically coupled transfer arm. The mu-metal analysis chamber was equipped with an Omicron Sphera-II electrostatic analyzer for photoemission spectroscopy. For x-ray photoemission spectroscopy (XPS) a Mg/Al dual anode x-ray source and for ultraviolet photoemission spectroscopy (UPS) a VUV He-discharge lamp was used. The analysis chamber also hosts a room temperature scanning tunneling microscope (STM) (Omicron STM 1). Additional analysis was performed in a separate variable temperature STM that allowed cooling of the sample to 15 K with a closed-cycle cryostat. The samples were transferred into the variable temperature STM in a vacuum suitcase without exposing them to air. The pressure in the vacuum suitcase was maintained at  $\sim 10^{-8}$  Torr with an ion getter pump during transfer. STM imaging and local STS was acquired with a cut PtIr- tip. For dI/dV spectroscopy a lock-in amplifier with a modulation voltage of 7 mV and reference frequency of 995 Hz was used. Finally, for a few selected samples Micro-ARPES measurements were performed at the ANTARES beamline in SOLEIL synchrotron in France. The beam spot size was  $\sim 120 \mu m$ . The angular and energy resolution of the beamline at a photon energy of 40 eV are  $\sim 0.2^{\circ}$  and  $\sim 10 \text{ meV}$ , respectively. All ARPES data were collected with the sample at 300 K.

### 4. Results and discussion

MoSe<sub>2</sub> films are grown by MBE on van der Waals substrates and characterized without exposure to air. In addition, MoSe<sub>2</sub> films could also be doped with Te by co-deposition of Se and Te. Samples were characterized by XPS, UPS, scanning tunneling microscopy and spectroscopy at the University of South Florida as well as by ARPES at the ANTARES beamline at SOLEIL synchrotron in France. We first concentrate on the question how the van der Waals substrate influences the electronic structure of MoSe<sub>2</sub>. Then, how Se

 IOP Publishing
 2D Mater. 4 (2017) 025094
 H C Diaz et al

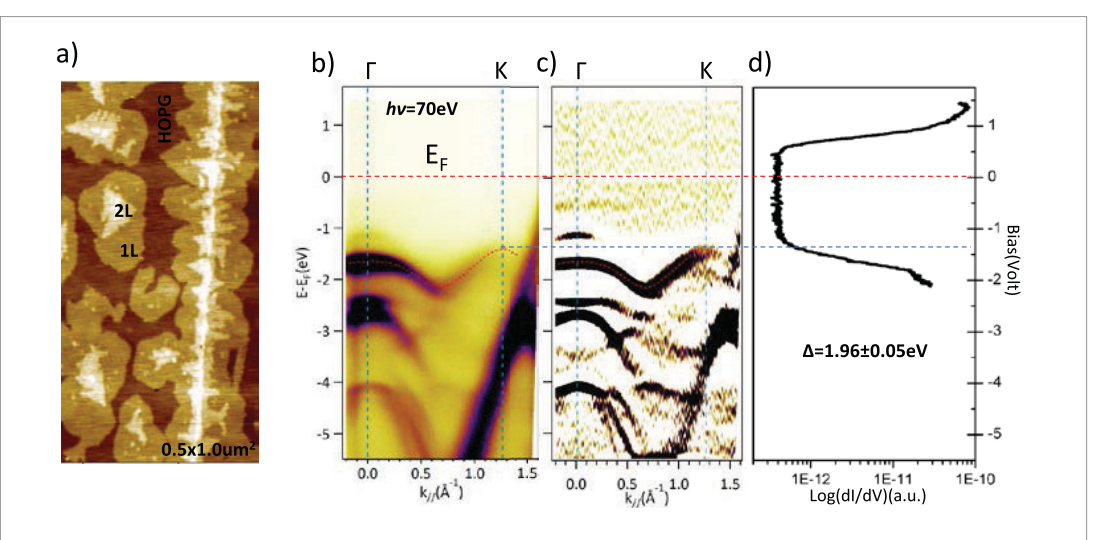


**Figure 1.** Electronic structure of MoSe<sub>2</sub> film on HOPG. (a) AFM images of MoSe<sub>2</sub>, the areas labeled with 1 L, and 2 L indicate monoand bi- layers of MoSe<sub>2</sub>, respectively. (b) ARPES spectrum of MoSe<sub>2</sub> on HOPG along  $\Gamma$ -K direction. (c) Second derivative of the ARPES spectra shown in (b). (d) STS spectrum of mono-layer of MoSe<sub>2</sub> on HOPG.

substitution by Te affects the stability and electronic structure.

### 4.1. Electronic structure of MoSe<sub>2</sub> on HOPG-versus MoS<sub>2</sub>- substrates

MoSe $_2$  has been grown on HOPG- and MoS $_2$ - substrates. While the MoS $_2$  substrate was single crystalline, HOPG is naturally polycrystalline, however, the grains are large enough to enable micro-ARPES measurements. The main question we want to address in this study is the influence of the substrate on the electronic structure of MoSe $_2$ . The conductive nature of HOPG may cause a strong band renormalization, i.e. narrowing of the band gap compared to free-standing MoSe $_2$ , while for MoSe $_2$ /MoS $_2$  heterostructure hybridization of chalcogen states at the  $\Gamma$ -point may result in a band edge modifications compared to free-standing MoSe $_2$ .

Large scale ambient air atomic force microscopy images of MoSe<sub>2</sub> grown on HOPG, shown in figure 1(a), indicate the preferential nucleation and growth at step edges. Before completion of the first layer, the second layer nucleates and thus ARPES measurements show a mixture of single- and bi-layer MoSe2. It is well established that only the monolayer of MoSe<sub>2</sub> has a direct band gap at the K-point and that for bilayer the VBedge at the  $\Gamma$ -point is lower in binding energy than that at the K-point. This behavior is reproduced in the ARPES data shown in figure 1(b). Since both mono- and bi-layer are measured simultaneously the ARPES data shows a superpositioning of the electronic structure of both. Since the monolayer coverage is much larger than the bilayer region the ARPES spectra is dominated by the monolayer and the bilayer region only contributes weakly. Nevertheless, at the  $\Gamma$ -point we resolve two bands. A strong intensity band with at a binding energy of 1.64 eV, which is assigned to the monolayer regions and a faint band at a binding energy of 1.14 eV, which is assigned to the bilayer region. Thus, we measure a

shift of the VBM from the monolayer to the bilayer at the  $\Gamma$ -point of 0.5 eV. This agrees well with previously reported differences of the VBM at the  $\Gamma$ -point of ~0.47 eV in ARPES measurements for mono- and bilayer materials [56]. Importantly, for the monolayer the VBM at the  $\Gamma$ -point is around ~0.23 eV below the VBM at the K-point, while for the bilayer, the VBM is ~0.27 eV above the VBM at the K-point, assuming the K-point is the same for mono- and bi-layer MoSe<sub>2</sub>. Furthermore, the band shape at the  $\Gamma$ -point is relatively flat for the monolayer, indicating a higher effective mass for holes in the monolayer than for bi-layer or bulk MoSe<sub>2</sub>. From a parabolic fit of the band at the  $\Gamma$ -point we estimate an effective mass of  $3.07 \pm 0.08$  m<sub>e</sub> for monolayer MoSe<sub>2</sub> on HOPG. Photoemission only probes the filled states, thus to obtain information of the band gap we performed STS on monolayer MoSe<sub>2</sub> on HOPG, shown in figure 1(d). The binding energy of the VBM agrees well with the ARPES data and the CBM is measured at ~0.5 eV above the Fermi-level indicating an n-type doping of the MoSe<sub>2</sub> monolayer. The band gap determined from STS is  $\sim$  1.96  $\pm$  0.05 eV. This is  $\sim$  10% smaller than the band gap reported for MoSe<sub>2</sub> on bilayer graphene/ SiC of 2.16 eV [60]. This smaller band gap of MoSe<sub>2</sub> monolayer on HOPG may be a consequence of a larger band renormalization on HOPG compared to graphene.

Now we turn to single layer MoSe<sub>2</sub> grown on MoS<sub>2</sub> substrates. On MoS<sub>2</sub>, MoSe<sub>2</sub> nucleates more uniformly (it still maybe a heterogeneous nucleation process, but MoS<sub>2</sub> may have more nucleation sites than HOPG), and thus a more homogeneously covered surface is obtained with almost complete monolayer and only small fraction of bilayer as the *in situ* STM image in figure 2(a) shows. Consequently, the ARPES data in figures 2(b) and (c) is almost entirely from the single layer MoSe<sub>2</sub> and contribution of second layer is almost negligible. Also, the photon energy of 70 eV is extreme surface sensitive and thus most of the sig-

2D Mater. 4 (2017) 025094 H C Diaz et al

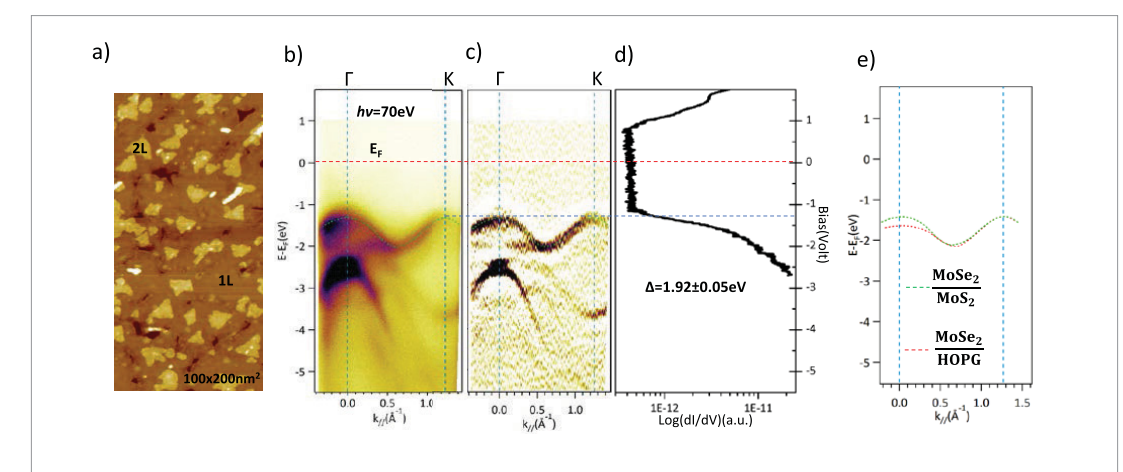


Figure 2. Electronic structure of mono-layer of  $MoSe_2$  on  $MoS_2$ . (a) Large scale STM imagen of  $MoSe_2$ , mono- and bi-layers of  $MoSe_2$  are labeled with 1 L and 2 L, respectively. (b) ARPES spectrum for  $MoSe_2$  on  $MoS_2$  along  $\Gamma$ –K direction. (c) Second derivative of data in panel (a). (d) STS spectrum of mono-layer of  $MoSe_2$ . (e) Comparison between the VBM for  $MoSe_2$  grown on  $MoSe_2$  grown on  $MoSe_2$  grown on  $MoSe_3$ .

nal is from the MoSe<sub>2</sub> surface layer. For this sample, we measure the VBM at almost the same binding energy at the  $\Gamma$ - and K- points. Very weak contribution from the 2nd layer islands can be found at smaller binding energy at the  $\Gamma$ -point. Fitting a parabolic dispersion to the VBM at the  $\Gamma$ -point allows us to estimate the effective mass to 0.82  $\pm$  0.01  $m_{\rm e}$ . STS measurements, shown in figure 2(d), of this sample indicates a band gap of 1.92  $\pm$  0.05 eV.

IOP Publishing

There are clear differences in the band structure of single layer MoSe<sub>2</sub> on HOPG compared to MoS<sub>2</sub> as summarized by the VBM traces for MoSe2 on these two substrates, shown in figure 2(e). This variation of the electronic structure indicates differences in the substrate interactions. A flatter band of MoSe<sub>2</sub> monolayers at  $\Gamma$  on a HOPG- compared to a MoS<sub>2</sub>- substrate is consistent with retaining the properties of freestanding MoSe<sub>2</sub>, i.e. weak interlayer hybridization. The significantly lower binding energy of the VBM at  $\Gamma$  compared to K also agrees with the expectations for free-standing MoSe<sub>2</sub>. Thus, the main difference between free-standing MoSe<sub>2</sub> and MoSe<sub>2</sub>/HOPG is a reduced band gap due to bandgap renormalization by the conducting substrate. In contrast, MoSe<sub>2</sub> on MoS<sub>2</sub> has its VBM at  $\Gamma$  raised to almost the same energy as the VBM at K. Furthermore, it disperses more than expected for freestanding MoSe<sub>2</sub>. These effects can be attributed to hybridization of the Se p-states with the S p-states from the substrate. In bilayer or bulk hybridization of chalcogen p-states at the  $\Gamma$ -point are partially responsible for the change from a direct to an indirect band gap due to the lowering of the binding energy and thus raising the VBM at  $\Gamma$ - above the VBM at the K-point. For the MoSe<sub>2</sub>/MoS<sub>2</sub> heterostructure, it appears that the hybridization is not as strong and only raises the VBM for MoSe<sub>2</sub> at the  $\Gamma$ -point roughly to the same energy as the VBM at K. Such a hybridization also changes the dispersion of the  $\Gamma$ -point, resulting in significantly lower effective mass compared to MoSe<sub>2</sub> on HOPG. Finally, hybridization of electronic

states suggests that these states overlap in momentum and energy. This would imply that the MoSe<sub>2</sub> p-derived band is energetically aligned with the MoS<sub>2</sub> p-states of the substrate. This effect cannot be clearly seen for the full monolayer film at the used photon energy because the substrate bands are not visible. The alignment of the monolayer VBM binding energy to those of the substrate at the  $\Gamma$ -point is better seen on the samples discussed in the next section because they only exhibit a partial monolayer and thus both substrate and monolayer are observed in the same spectrum.

### 4.2. Properties of $MoSe_{2(1-x)}Te_{2x}$

The flexibility of MBE in co-deposition of different elements also enables in principle the direct growth of solid solutions of isostructural TMDCs and thus the tuning of the properties of TMDC monolayers. There already exist a few studies that examine the properties of solid solution TMDCs. For example, for the  $MoS_xSe_{2-x}$ system it has been shown that by changing the S to Se ratio the photoluminescence, i.e. the optical gap can be continuously tuned between the values of the pure chalcogenides [71–77]. In addition of tuning gaps, alloying may also affect the chemical stability. Generally, air-stability and aging of synthesized monolayer materials is a concern for TMDCs [78]. Often the chemical stability of materials correlates with the band gap, with wide band gap materials being more stable than narrow band gap or metals. This is certainly also the case for Mo-chalcogenides, with the chemical (air) stability decreasing in the order of MoS<sub>2</sub>, MoSe<sub>2</sub>, to MoTe<sub>2</sub>. MoTe<sub>2</sub> easily oxidize if exposed to air [29] while both MoS<sub>2</sub> and MoSe<sub>2</sub> monolayers are stable in air at room temperature for some time, but eventually also start to degrade. Step edges or defects in these materials are likely the starting points for such degradation.

To investigate chemical stability of Te-doped MoSe<sub>2</sub> and the electronic properties of doped samples we have grown MoSe<sub>2(1-x)</sub>Te<sub>2x</sub> samples by co-evaporation of

 IOP Publishing
 2D Mater. 4 (2017) 025094
 H C Diaz et al

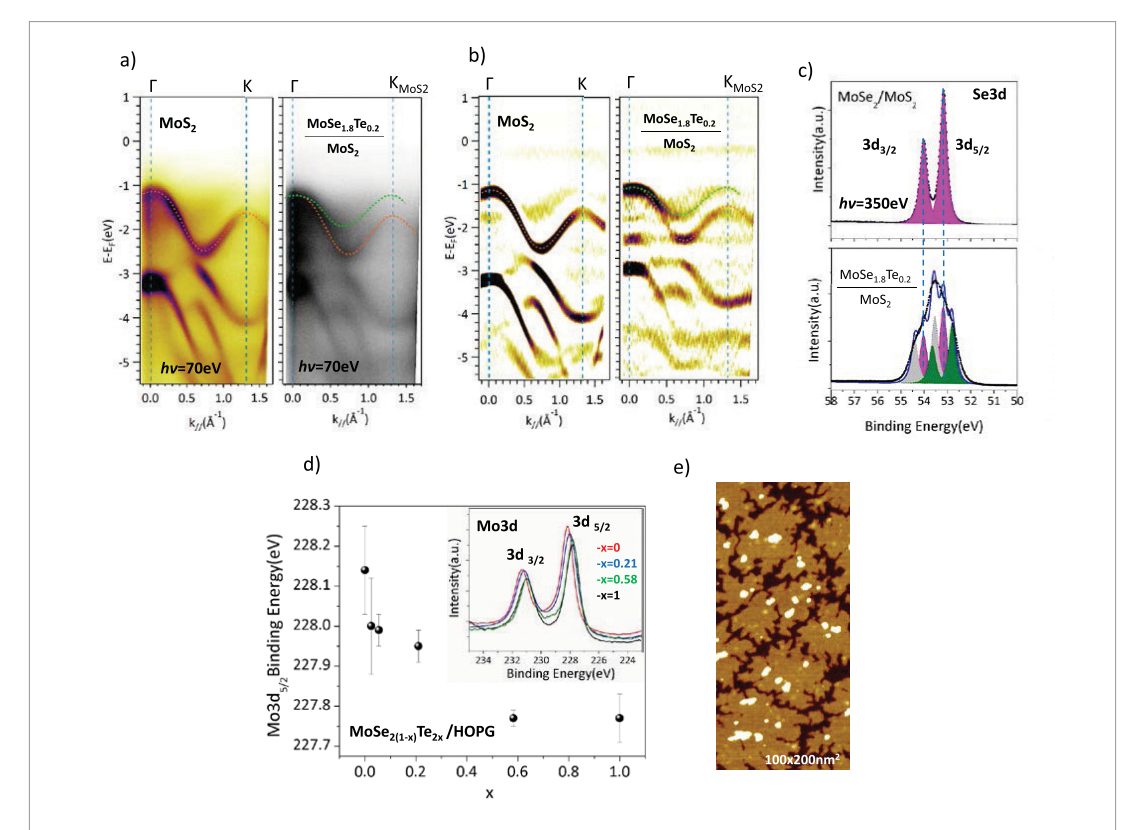


**Figure 3.** Properties of  $MoSe_{2(1-x)}Te_{2x}$ . (a) ARPES spectra for bulk  $MoS_2$ -substrate and sub-monolayer film of  $MoSe_{1.8}Te_{0.2}$  on  $MoS_2$ , along  $\Gamma$ – $K_{MoS_2}$  direction. (b) Second derivative of the ARPES data shown in panel (a). (c) High resolution synchrotron Se-3d core level data taken with 350 eV photon energy for pure  $MoSe_2$  and  $MoSe_{1.8}Te_{0.2}$  film on  $MoS_2$ . (d) Mo-3d core level binding energy measured with a lab XPS source of  $MoSe_{2(1-x)}Te_{2x}$  samples with different concentration of Te. Some XPS Mo-3d spectra are shown in the inset, the Mo3d Mo2 peak position is shifting to lower binding energy with the increasing Te concentration. (e) Large scale STM imagen of the  $MoSe_{1.8}Te_{0.2}$  film on  $MoS_2$ .

Se and Te.  $MoTe_2$  has different phases including the 2H-structure of  $MoSe_2$ . Thus, the mixed  $MoSe_{2(1-x)}Te_{2x}$  is expected to be a solid solution of  $MoSe_2$  and 2H- $MoTe_2$ . Addition of Se to  $MoTe_2$  stabilizes the semiconducting 2H phase and suppress the formation of metallic 1T or 1T' phases. In previous studies of MBE growth of pure  $MoTe_2$  we found that small amounts of the 1T' phase was present, predominantly at edges of grown islands [29]. We also found that these MBE grown  $MoTe_2$  films were very reactive and easily oxidized upon exposure to air. The metallic edges may contribute to the ready oxidation. Here, we found that addition of Se makes these films more chemically stable in air, possibly due to a suppression of a 1T' phase formation.

We performed ARPES measurements on a single  $MoSe_{2(1-x)}Te_{2x}$  sample with about 10% Te, i.e.  $MoSe_{1.8}Te_{0.2}$ . Surprisingly, the band that comprises the VBM appeared very similar compared to pure  $MoSe_2$  in the ARPES data. Figure 3(a), shows ARPES of the  $MoS_2$  substrate and for submonolayer of  $MoSe_{1.8}Te_{0.2}$ . The submonolayer amount of  $MoSe_{1.8}Te_{0.2}$  allows us to see both the signal from the substrate as well as the monolayer. It is apparent that the VBM of the monolayer and the  $MoS_2$  substrate overlap at the  $\Gamma$ -point, which strengthens the suggestion that this overlap enables the hybridization of these states and effectively aligns the  $\Gamma$ -point of the monolayer to the binding energy of the

 $\Gamma$ -point of the MoS<sub>2</sub> substrate. This alignment of the binding energies of the VBM at the  $\Gamma$ -point may contribute to the very similar VB for the MoSe<sub>1.8</sub>Te<sub>0.2</sub> sample as for the pure MoSe<sub>2</sub> monolayer on MoS<sub>2</sub> substrates.

Te is less electronegative than Se, which is responsible for the chemical shift of the Mo core levels from 228.14 eV to 227.77 eV as the composition is changed from pure MoSe<sub>2</sub> to pure MoTe<sub>2</sub>. Figure 3(d) shows the change in the core-level position as a function of Te-doping. Interestingly the Mo-peak appears to shift rigidly without indication of a significant broadening or even multiple components that could be associated with different number of Se and Te ligands to each Moatom. While there is a clear peak shift for Mo, the Se and Te peak position remains almost unaltered within the resolution limit of our laboratory XPS. High resolution synchrotron core level data taken with 350 eV photon energy for pure MoSe<sub>2</sub> and MoSe<sub>1.8</sub>Te<sub>0.2</sub> indicate however a peak broadening of the Se peak after incorporation of ~10% Te into MoSe<sub>2</sub>. While for pure MoSe<sub>2</sub> the Se can be fit with a single spin-orbit split core level doublet, after Te incorporation the Se peak requires at least 3 doublets for obtaining a reasonable fit. Such broadening indicates that the Se core level shows some sensitivity to the local environment and dependence on the number of Te-ligands to the adjacent Mo-atom.

### 5. Conclusions

Recent interest in van der Waals heterostructures has sparked renewed research efforts in van der Waals epitaxy by MBE of layered TMDCs, which enables the combination of materials with diverse properties regardless of their lattice matching. Many van der Waals materials grow epitaxially, i.e. the grown layers are in rotational registry with that of a van der Waals substrate. This enables, for example, ARPES measurements for MoSe<sub>2</sub> films on MoS<sub>2</sub> single crystal substrates. ARPES data indicates that the valence band maximum of MoSe<sub>2</sub> is modified depending on the substrate. On MoS<sub>2</sub> substrates, the VBM at the  $\Gamma$ -point is almost at the same binding energy as at the K-point for monolayer MoSe2. In contrast, on HOPG the difference in binding energy of the VBM at  $\Gamma$ - and K-points is similar to that expected for freestanding monolayer MoSe<sub>2</sub>. This difference may be understood in terms of hybridization between the chalcogen p-orbitals of the substrate with those of the monolayer. This hybridization of monolayer with that of the substrate also results in an alignment of the VBM at the  $\Gamma$ -point of the MoSe<sub>2</sub> monolayer to the binding energy of the VBM position of MoS<sub>2</sub>. No such alignment of binding energies is observed for MoSe<sub>2</sub> on HOPG. The hybridization of the MoSe<sub>2</sub> monolayer with the MoS<sub>2</sub> substrate is also reflected by the band dispersion, which shows a more bulk-like dispersion of the VBM at the  $\Gamma$ -point. The different properties of MoSe<sub>2</sub> monolayers depending on the substrate clearly shows that interlayer interactions need to be considered in defining the properties of van der Waals heterostructures.

### Acknowledgment

The authors acknowledge support from the National Science Foundation under Award DMR-1701390 and ECCS-1608654. The Synchrotron SOLEIL is supported by the Centre National de la Recherche Scientifique (CNRS) and the Commissariat à l'Energie Atomique et aux Energies Alternatives (CEA), France.

### References

- [1] Novoselov K S, Mishchenko A, Carvalho A and Castro Neto A H 2016 2D materials and van der Waals heterostructures *Science* 353 461
- [2] Jariwala D, Sangwan V K, Lauhon L J, Marks T J and Hersam M C 2014 Emerging device applications for semiconducting two-dimensional transition metal dichalcogenides ACS Nano 8 1102–20
- [3] Koma A 1999 Van der Waals epitaxy for highly latticemismatched systems J. Cryst. Growth 201 236
- [4] Geim A K and Grigorieva IV 2013 Van der Waals heterostructures Nature 499 419–25
- [5] Dean C R et al 2013 Hofstadter's butterfly and the fractal quantum Hall effect in moiré superlattices Nature 497 598–602
- [6] Ponomarenko L A et al 2013 Cloning of Dirac fermions in graphene superlattices Nature 497 594–7

- [7] Ma Q et al 2016 Tuning ultrafast electron thermalization pathways in a van der Waals heterostructure Nat. Phys. 12 455
- [8] Liu C H, Clark G, Fryett T, Wu S F, Zheng J J, Hatami F, Xu X D and Majumdar A 2017 Nanocavity integrated van der Waals heterostructure light-emitting tunneling diode *Nano Lett*. 17 200–5
- [9] Vu Q A et al 2017 Tuning carrier tunneling in van der Waals heterostructures for ultrahigh detectivity Nano Lett. 17 453–9
- [10] Wang F, Wang Z, Xu K, Wang F, Wang Q, Huang Y, Yin L and He J 2015 Tunable GaTe-MoS<sub>2</sub> van der Waals p-n junctions with novel optoelectronic performance Nano Lett. 15 7558–66
- [11] Padilha J E, Fazzio A and da Silva A J R 2015 van der Waals heterostructure of phosphorene and graphene: tuning the schottky barrier and doping by electrostatic gating *Phys. Rev. Lett.* 114 066803
- [12] Huo N J, Kang J, Wei Z M, Li S S, Li J B and Wei S H 2014 Novel and enhanced optoelectronic performances of multilayer MoS<sub>2</sub>–WS<sub>2</sub> heterostructure transistors Adv. Funct. Mater. 24 7025–31
- [13] Lopez-Sanchez O, Llado E A, Koman V, Morral A F I, Radenovic A and Kis A 2014 Light generation and harvesting in a van der Waals heterostructure ACS Nano 8 3042–8
- [14] Schaibley J R, Rivera P, Yu H Y, Seyler K L, Yan J Q, Mandrus D G, Taniguchi T, Watanabe K, Yao W and Xu X D 2016 Directional interlayer spin-valley transfer in twodimensional heterostructures Nat. Commun. 7 13747
- [15] Chen H L et al 2016 Ultrafast formation of interlayer hot excitons in atomically thin MoS<sub>2</sub>/WS<sub>2</sub> heterostructures Nat. Commun. 7 12512
- [16] Peng B, Yu G N, Liu X F, Liu B, Liang X, Bi L, Deng L I, Sum T C and Loh K P 2016 Ultrafast charge transfer in MoS<sub>2</sub>/WSe<sub>2</sub> p-n heterojunction 2D Mater. 3 025020
- [17] Rivera P, Seyler K L, Yu H Y, Schaibley J R, Yan J Q, Mandrus D G, Yao W and Xu X D 2016 Valley-polarized exciton dynamics in a 2D semiconductor heterostructure *Science* 351 688–91
- [18] Rivera P et al 2015 Observation of long-lived interlayer excitons in monolayer MoSe<sub>2</sub>-WSe<sub>2</sub> heterostructures Nat. Commun. 6 6242
- [19] Fang H et al 2014 Strong interlayer coupling in van der Waals heterostructures built from single-layer chalcogenides Proc. Natl Acad. Sci. USA 111 6198–202
- [20] Samad L, Bladow S M, Ding Q, Zhuo J Q, Jacobberger R M, Arnold M S and Jin S 2016 Layer-controlled chemical vapor deposition growth of MoS<sub>2</sub> vertical heterostructures via van der Waals epitaxy ACS Nano 10 7039–46
- [21] Choudhary N, Park J, Hwang J Y, Chung H S, Dumas K H, Khondaker S I, Choi W B and Jung Y 2016 Centimeter Scale Patterned Growth of Vertically Stacked Few Layer Only 2D MoS<sub>2</sub>/WS<sub>2</sub> van der Waals Heterostructure Sci. Rep. 6 25456
- [22] Zhang Q, Chen Y X, Zhang C D, Pan C R, Chou M Y, Zeng C G and Shih C K 2016 Bandgap renormalization and work function tuning in MoSe<sub>2</sub>/hBN/Ru(0001) heterostructures *Nat. Commun.* 7 13843
- [23] Zhao M, Liu M M, Dong Y Q, Zou C, Yang K Q, Yang Y, Zhang L J and Huang S M 2016 Epitaxial growth of twodimensional SnSe<sub>2</sub>/MoS<sub>2</sub> misfit heterostructures J. Mater. Chem. C 4 10215–22
- [24] Ben Aziza Z, Henck H, Pierucci D, Silly M G, Lhuillier E, Patriarche G, Sirotti F, Eddrief M and Ouerghi A 2016 van der Waals epitaxy of GaSe/graphene heterostructure: electronic and interfacial properties ACS Nano 10 9679–86
- [25] Aretouli K E, Tsoutsou D, Tsipas P, Marquez-Velasco J, Giamini S A, Kelaidis N, Psycharis V and Dimoulas A 2016 Epitaxial 2D SnSe<sub>2</sub>/2D WSe<sub>2</sub> van der Waals heterostructures ACS Appl. Mater. Interfaces 8 23222–9
- [26] Li X F et al 2016 Two-dimensional GaSe/MoSe $_2$  misfit bilayer heterojunctions by van der Waals epitaxy Sci. Adv. 2 e1501882
- [27] Tsoutsou D, Aretouli K E, Tsipas P, Marquez-Velasco J, Xenogiannopoulou E, Kelaidis N, Giamini S A and Dimoulas A 2016 Epitaxial 2D MoSe<sub>2</sub> (HfSe<sub>2</sub>) semiconductor/2D TaSe<sub>2</sub> metal van der Waals heterostructures ACS Appl. Mater. Interfaces 8 1836–41

- [28] Liu X L, Balla I, Bergeron H, Campbell G P, Bedzyk M J and Hersam M C 2016 Rotationally commensurate growth of MoS<sub>2</sub> on epitaxial graphene ACS Nano 10 1067–75
- [29] Coy Diaz H, Chaghi R, Ma Y and Batzill M 2015 Molecular beam epitaxy of the van der Waals heterostructure MoTe<sub>2</sub> on MoS<sub>2</sub>: phase, thermal, and chemical stability 2D Mater. 2 044010
- [30] Li X F et al 2015 Van der Waals epitaxial growth of twodimensional single-crystalline GaSe domains on graphene ACS Nano 9 8078–88
- [31] Vishwanath S et al 2015 Comprehensive structural and optical characterization of MBE grown MoSe<sub>2</sub> on graphite, CaF<sub>2</sub> and graphene 2D Mater. 2 024007
- [32] Miwa J A, Dendzik M, Gronborg S S, Bianchi M, Lauritsen J V, Hofmann P and Ulstrup S 2015 Van der Waals epitaxy of twodimensional MoS<sub>2</sub>-graphene heterostructures in ultrahigh vacuum ACS Nano 9 6502–10
- [33] Jiao L et al 2015 Molecular-beam epitaxy of monolayer MoSe<sub>2</sub>: growth characteristics and domain boundary formation New J. Phys. 17 053023
- [34] Yuan X *et al* 2015 Arrayed van der Waals vertical heterostructures based on 2D GaSe grown by molecular beam epitaxy *Nano Lett.* **15** 3571–7
- [35] Aretouli K E, Tsipas P, Tsoutsou D, Marquez-Velasco J, Xenogiannopoulou E, Giamini S A, Vassalou E, Kelaidis N and Dimoulas A 2015 Two-dimensional semiconductor HfSe<sub>2</sub> and MoSe<sub>2</sub>/HfSe<sub>2</sub> van der Waals heterostructures by molecular beam epitaxy Appl. Phys. Lett. 106 143105
- [36] Yan A, Velasco J Jr, Kahn S, Watanabe K, Taniguchi T, Wang F, Crommie M F and Zettl A 2015 Direct growth of single- and few-layer MoS<sub>2</sub> on h-BN with preferred relative rotation angles Nano Lett. 15 6324–31
- [37] Robinson J A 2016 Growing vertical in the flatland ACS Nano 10 42–5
- [38] Huang C, Wu S, Sanchez A M, Peters J J P, Beanland R, Ross J S, Rivera P, Yao W, Cobden D H and Xu X 2014 Lateral heterojunctions within monolayer MoSe<sub>2</sub>–WSe<sub>2</sub> semiconductors Nat. Mater. 13 1096–101
- [39] Duan X et al 2014 Lateral epitaxial growth of two-dimensional layered semiconductor heterojunctions Nat. Nanotechnol. 9 1024–30
- [40] Lv R, Robinson J A, Schaak R E, Sun D, Sun Y, Mallouk T E and Terrones M 2015 Transition metal dichalcogenides and beyond: synthesis, properties, and applications of single- and few-layer nanosheets Acc. Chem. Res. 48 56–64
- [41] Koma A 1992 Van der Waals epitaxy- a new epitaxial growth method for a highly lattice mismatched system *Thin Solid Films* 216 72–6
- [42] Ohuchi F S, Parkinson B A, Ueno K and Koma A 1990 van der Waals epitaxial growth and characterization of MoSe<sub>2</sub> thin films on SnS<sub>2</sub> J. Appl. Phys. 68 2166–75
- [43] Ueno K, Takeda N, Sasaki K and Koma A 1997 Investigation of the growth mechanism of layered GaSe Appl. Surf. Sci. 113/4 38–42
- [44] Ohuchi F S, Shimada T, Parkinson B A, Ueno K and Koma A 1991 Growth of MoSe<sub>2</sub> thin films with Van der Waals epitaxy J. Cryst. Growth 111 1033–7
- [45] Schlaf R, Tiefenbacher S, Lang O, Pettenkofer C and Jaegermann W 1994 van der Waals epitaxy of thin InSe<sub>2</sub> films on MoTe<sub>2</sub> Surf. Sci. 303 L343-7
- [46] Yamada H, Ueno K and Koma A 1996 Preparation of GaS thin films by molecular beam epitaxy Japan. J. Appl. Phys. 35 L568–70
- [47] Lang O, Schlaf R, Tomm Y, Pettenkofer C and Jaegermann W 1994 Single crystalline GaSe/WSe<sub>2</sub> heterointerface grown by van der Waals epitaxy. I. Growth conditions J. Appl. Phys. 75 7805–13
- [48] Schlaf R, Lang O, Pettenkofer C and Jaegermann W 1999 Band lineup of layered semiconductor heterointerfaces prepared by van der Waals epitaxy: charge transfer correction term for the electron affinity rule J. Appl. Phys. 85 2732–53
- [49] Lang O, Klein A, Pettenkofer C, Jaegermann W and Chevy A 1996 Band lineup of lattice mismatched InSe/GaSe quantum

- well structures prepared by van der Waals epitaxy: absence of interfacial dipoles *J. Appl. Phys.* **80** 3817–21
- [50] Schlaf R, Pettenkofer C and Jaegermann W 1999 Band lineup of SnS<sub>2</sub>/SnSe<sub>2</sub>/SnS<sub>2</sub> semiconductor quantum well structure prepared by van der Waals epitaxy J. Appl. Phys. 85 6550–6
- [51] Kreis C, Traving M, Adelung R, Kipp L and Skibowski M 2000 Tracing the valence band maximum during epitaxial growth of HfS<sub>2</sub> and WSe<sub>2</sub> Appl. Surf. Sci. 166 17–22
- [52] Kreis C, Werth S, Adelung R, Kipp L, Skibowski M, Voss D, Krueger P, Mazur A and Pollmann J 2002 Surface resonances at transition metal dichalcogenide heterostructures *Phys. Rev.* B 65 153314
- [53] Klein A, Tiefenbacher S, Eyert V, Pettenkofer C and Jaergermann W 2001 Electronic band structure of singlecrystal and single-layer WSe<sub>2</sub>: influence of interlayer van der Waals interactions *Phys. Rev.* B 64 205416
- [54] Mak K F, Lee C, Hone J, Shan J and Heinz T F 2010 Atomically thin MoS<sub>2</sub>: a new direct-gap semiconductor *Phys. Rev. Lett.* 105 136805
- [55] Jin W C et al 2013 Direct measurement of the thicknessdependent electronic band structure of MoS<sub>2</sub> using angleresolved photoemission spectroscopy Phys. Rev. Lett. 111 106801
- [56] Zhang Y et al 2014 Direct observation of the transition from indirect to direct bandgap in atomically thin epitaxial MoSe<sub>2</sub> Nat. Nanotechnol. 9 111–5
- [57] Mo S K, Hwang C, Zhang Y, Fanciulli M, Muff S, Dil J H, Shen Z X and Hussain Z 2016 Spin-resolved photoemission study of epitaxially grown MoSe<sub>2</sub> and WSe<sub>2</sub> thin films J. Phys.: Condens. Matter 28 454001
- [58] Cheng Y, Zhua Z and Schwingenschlögl U 2012 Role of interlayer coupling in ultra thin MoS<sub>2</sub> RSC Adv. 2 7798–802
- [59] Bradley A J et al 2015 Probing the role of interlayer coupling and Coulomb interactions on electronic structure in few-layer MoSe<sub>2</sub> nanostructures Nano Lett. 15 2594–9
- [60] Ugeda M M et al 2014 Giant bandgap renormalization and excitonic effects in a monolayer transition metal dichalcogenide semiconductor Nat. Mater. 13 1091–5
- [61] Bruix A et al 2016 Single-layer MoS<sub>2</sub> on Au(111): band gap renormalization and substrate interaction Phys. Rev. B 93 165422
- [62] Diaz H C, Addou R and Batzill M 2014 Interface properties of CVD grown graphene transferred onto  $MoS_2(0001)$  Nanoscale 6 1071–8
- [63] Coy-Diaz H, Bertran F, Chen CY, Avila J, Rault J, Le Fevre P, Asensio M C and Batzill M 2015 Band renormalization and spin polarization of MoS<sub>2</sub> in graphene/MoS<sub>2</sub> heterostructures *Phys. Status Solidi RRL* 9 701–6
- [64] Kuc A, Zibouche N and Heine T 2011 Influence of quantum confinement on the electronic structure of the transition metal sulfide TS<sub>2</sub> Phys. Rev. B 83 245213
- [65] Tiefenbacher S, Pettenkofer C and Jaegermann W 2000 Moiré pattern in LEED obtained by van der Waals epitaxy of lattice mismatched WS<sub>2</sub>/MoTe<sub>2</sub>(0001) heterointerfaces Surf. Sci. 450 181–90
- [66] Terrones H, López-Urías F and Terrones M 2013 Novel hetero-layered materials with tuneable direct band gaps by sandwiching different metal disulfides and diselenides Sci. Rep. 3 1549
- [67] Kang J, Li J, Li S-S, Xia J-B M and Wang L-W 2013 Electronic structural moiré pattern effects on MoS<sub>2</sub>/MoSe<sub>2</sub> 2D heterostructures Nano Lett. 13 5485–90
- [68] Zhang C, Chuu C-P, Ren X, Li M-Y, Li L-J, Jin C, Chou M-Y and Shih C-K 2017 Interlayer couplings, Moiré patterns, and 2D electronic superlattices in MoS<sub>2</sub>/WSe<sub>2</sub> hetero-bilayers Sci. Adv. 3 e1601459
- [69] Wilson N R et al 2017 Determination of band offsets, hybridization, and exciton binding in 2D semiconductor heterostructures Sci. Adv. 3 e1601832
- [70] Coy Diaz H, Avila J, Chen C, Addou R, Asensio M C and Batzill M 2015 Direct observation of interlayer hybridization and Dirac relativistic carriers in graphene/MoS<sub>2</sub> van der Waals heterostructures Nano Lett. 15 1135–40

- [71] Feng Q, Mao N, Wu J, Xu H, Wang C, Zhang J and Xie L 2015 Growth of  $MoS_{2(1-x)}Se_{2x}(x=0.41-1.00)$  monolayer alloys with controlled morphology by physical vapor deposition ACS Nano 9 7450–5
- [72] Feng Q et al 2014 Growth of large-area 2D MoS $_{2(1-x)}$ Se $_{2x}$  semiconductor alloys Adv. Mater. 26 2648–53
- [73] Umrao S, Jeon J, Jeon S M, Choi Y J and Lee S 2017 A homogeneous atomic layer MoS<sub>2(1-x)</sub>Se<sub>2x</sub> alloy prepared by low-pressure chemical vapor deposition, and its properties *Nanoscale* **9** 594–603
- [74] Rajbanshi B, Sarkar S and Sarkar P 2015 The electronic and optical properties of  $MoS_{2(1-x)}Se_{2x}$  and  $MoS_{2(1-x)}Te_{2x}$  monolayers *Phys. Chem. Chem. Phys.* **17** 26166
- [75] Yang L, Fu Q, Wang W, Huang J, Huang J, Zhang J and Xiang B 2015 Large-area synthesis of monolayered  $MoS_{2(1-x)}Se_{2x}$  with a tunable band gap and its enhanced electrochemical catalytic activity Nanoscale 7 10490–7
- [76] Mann J et al 2014 2 dimensional transition metal dichalcogenides with tunable direct band gaps:  $MoS_{2(1-x)}Se_{2x}$  monolayers Adv. Mater. 26 1399–404
- [77] Kang J, Tongay S, Li J and Wu J 2013 Monolayer semiconducting transition metal dichalcogenide alloys: stability and band bowing J. Appl. Phys. 113 143703
- [78] Gao J, Li B, Tan J, Chow P, Lu T-M and Koratkar N 2016 Aging of transition metal dichalcogenide monolayers ACS Nano 10 2628–35